Proceedings of the ASME 2010 International Design Engineering Technical Conferences & Computers and Information in Engineering Conference
IDETC/CIE 2010
August 15-18, 2010, Montreal, Quebec, Canada

DETC2010/MECH-28673

THE KINEMATICS OF A-PAIR JOINTED SERIAL LINKAGES

James D. Robinson
Department of Mechanical and Aerospace Engineering
Carleton University
Ottawa, Ontario, Canada
Email: jrobins7@connect.carleton.ca

M. John D. Hayes*
Department of Mechanical and Aerospace Engineering
Carleton University
Ottawa, Ontario, Canada
Email: jhayes@mae.carleton.ca

ABSTRACT

A new kinematic pair called an algebraic screw pair, or A-pair, is introduced that utilizes the self-motions inherent to a specific configuration of Griffis-Duffy platform. Using the A-pair as a joint in a hybrid parallel-serial kinematic chain results in a sinusoidal coupling of rotation and translation between adjacent links. This motion affects both the direct and inverse kinematics of such chains. Presented in this paper are the direct kinematics of chains using A-pairs and an algorithm for the inverse kinematics of a 4A-pair chain.

INTRODUCTION

This paper introduces a novel kinematic pair that is intended to be used as a joint in a serial kinematic chain. The kinematic pair uses a specific configuration of a parallel manipulator called a Griffis-Duffy platform (GDP) which is a special configuration of Stewart-Gough platform (SGP) that, in most configurations, is subject to self-motions regardless of the state of the actuated legs. Self-motions represent situations where the end effector (EE) of the manipulator can move in an uncontrolled manner without actuator input. The rationale behind proposing this new kinematic pair, called an algebraic screw pair, or A-pair, is based on the hypothesis that replacing the revolute of a serial manipulator with this special configuration of parallel platform will enhance the rigidity of the serial arm. At the time of this writing, an actuated prototype 4A-chain is being designed and will be used to investigate the hypothesis. Hence, the focus of this paper is on the direct and inverse kinematics of short A-chains with one, two and four joints.

This paper details the special configuration of GDP that is used to construct the A-pair; presents the motion characteristics of the A-pair and describes how it is used as a joint in a kinematic chain; provides the direct kinematic equations of a serial chain constructed using any number of A-pairs; and presents an algorithm for solving the inverse kinematics problem for 4A-chains.

THE ALGEBRAIC SCREW PAIR

Before discussing the kinematics of A-chains, it is important to understand the geometry and motion characteristics of the individual A-pairs. This section describes the geometry of the GDP; the specific configuration of GDP that is used to create the A-pair; and how self-motions are utilized to turn the GDP into a kinematic pair.

The Griffis-Duffy Platform

In 1993 Griffis and Duffy [1] introduced a novel configuration of parallel manipulator called the Griffis-Duffy platform. A special configuration of the Stewart-Gough platform (six legged, six DOF parallel manipulator), the GDP is characterized by a planar fixed base and planar moving platform each with six specially placed spherical joint anchor points for the six legs of the manipulator. The six anchor points lie on the perimeter of a triangle on each of the fixed base and moving platform and six of the anchor points are located one on each of the vertices of the two triangles and the remaining six anchor points being located

*Address all correspondence to this author.

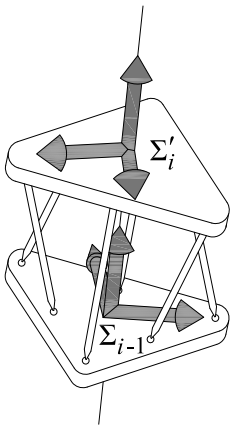

FIGURE 1. Example of a GDP. The configuration shown is called the midline-to-vertex configuration.

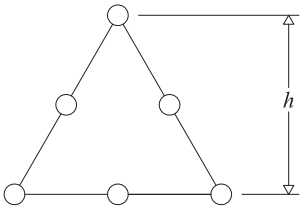

FIGURE 2. The height, h, of the congruent fixed base and moving platform triangles is equal to the distance from the anchor point at the midpoints of one of the sides of the triangle to the anchor point at the opposite vertex.

one on each edge of the triangles such that each leg has one anchor point on the fixed base and one anchor point on the moving platform. Fig. 1 shows one example of a GDP, many other configurations exist. Griffis and Duffy proposed controlling the EE of the manipulator (affixed to the moving platform) by controlling the length of each of the six legs. With this definition of the GDP configuration there are many possible configurations, however the work proposed here focuses on one particular configuration called the midline-to-vertex configuration, illustrated in Fig. 1, where a leg with an anchor point on the fixed base has an anchor point on the midpoint of one of the edges of the triangle on the moving platform and vice versa, maintaining the same order of legs around the perimeter of the fixed base and moving platform. Additionally the special GDP configuration used for the remainder of this paper has the following constraints applied: the fixed base and moving platform triangles are congruent equilateral triangles; and the six legs are all of a fixed length, l, equal to the height, h, of the triangles made by their anchor points (distance from the midpoint of one of the edges of the triangle to the opposite vertex on the same triangle, as illustrated in Fig. 2).

A significant issue with GDPs is self-motions. Self-motions represent instances where a manipulator can move in an uncontrolled manner without actuator input. For a GDP this means that the moving platform moves relative to the fixed base without changing the length of the legs. Husty and Karger have addressed the self-motions of Stewart-Gough platforms in general in [2] and [3] and have focused specifically on GDPs in [4], using the midline-to-vertex configuration as a detailed example. Husty and Karger show that the midline-to-vertex configuration of GDP, along with most other configurations of GDP, are always subject to self-motions regardless of the lengths of the actuated legs throughout the entire reachable workspace volume.

The GDP as a Kinematic Pair

Normally the existence of self-motions, especially throughout the entire reachable workspace, is an undesirable characteristic, thus the GDP is widely considered to be a failure as a parallel manipulator. An interesting characteristic of the midline-to-vertex GDP self-motions, as shown in [4], is that they possess one well-defined, uncontrollable degree-of-freedom (DOF). It turns out that the self-motions of the special GDP configuration described previously couple rotation about an axis passing through the geometric centres of both the fixed base and moving platform triangles with translation along that axis. The relationship between the rotation angle and the distance between the fixed base and moving platform is a simple trigonometric function.

The work presented in this paper uses the following relationship obtained by Husty and Karger [4] that describes the separation of the fixed base and moving platform, d, as a function of the rotation angle, θ, about the Z-axis common to both the fixed base and moving platform:

$$d = \rho \sin\left(\frac{\theta}{2}\right), \tag{1}$$

where ρ is a function of the geometry of the GDP. The current work focuses on a GDP constructed such that the fixed base and moving platform are congruent equilateral triangles with each side of the triangles being of length a. The length of the legs of the GDP, l, are held fixed and are equal to the height of the triangle such that

$$l = \frac{a\sqrt{3}}{2}. \tag{2}$$

The value of ρ obtained using this GDP geometry is

$$\rho = \frac{a\sqrt{6}}{3}. \tag{3}$$

When $\theta = 0^\circ$ the GDP is said to be in its *home position*. This is a theoretical position that can only be achieved if collisions between the physical elements that constitute the GDP are ignored, because in the home position $d = 0$ and the fixed base and moving platform are coincident. The home position is not physically accessable but is used as a reference position during kinematic analysis. When the platform is fully extended, similar to the pose shown in Fig. 1, $\theta = 180^\circ$ and $d = \rho$. This fully extended position, along with the geometry of the GDP, is used to determine the value of the constant ρ.

It is proposed in [5] to utilize the well-defined one DOF self-motion of this special GDP as a joint in a serial chain in place of standard revolute joints (R-pairs). The motivation behind this is that, beyond the rotation and translation about and along the joint axis, the truss-like structure of the parallel platform makes it very rigid in all other directions. This new type of joint, or kinematic pair, is called and algebraic screw pair (A-pair) because it is like a screw pair with the exception that the pitch of the screw can be represented as an algebraic function of the rotation angle (tangent of the half-angle substitution is used to represent the trigonometric function as an algebraic function).

The remainder of this paper presents the direct kinematics of chains constructed using A-pairs (A-chains) and introduces an algorithm for the inverse kinematics of A-chains with two and four joints (*i.e.* 2A- and 4A-chains).

DIRECT KINEMATICS OF A-CHAINS

Solving the direct kinematics problem for a known manipulator involves determining the position and orientation (pose) of the manipulator EE for a given set of joint variables. This section provides a solution to the direct kinematics problem by adapting well established methods. First the Denavit-Hartenburg (DH) parameters and a reference coordinate system are defined for each link in the A-chain and then the standard matrix form of the direct kinematics equations is adapted to account for the coupled rotation and translation of the A-pair.

Description of Joints and Links

DH-parameters are commonly used when studying serial manipulators to provide an unambiguous mathematical description of the kinematic chain. The interested reader is referred to Denavit and Hartenberg [6], Craig [7], Shigley and Uicker [8] or almost any reference on serial manipulator kinematics for a more detailed description of DH-parameters.

Four DH-parameters are used to unambiguously describe the kinematic geometry of each link in an n-link serial chain. For link i, where $i \in 1,\ldots,n$, the DH-parameters are defined as:

- the *link length*, a_i, is the length of the common normal between adjacent joint axes;

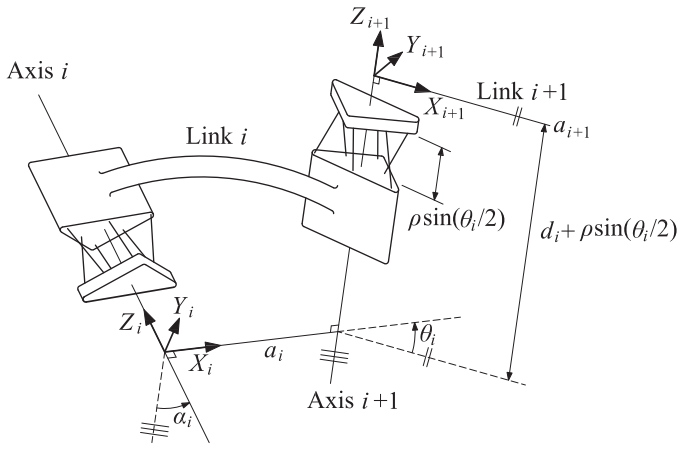

FIGURE 3. The DH-parameters for a link in an A-chain with appropriate coordinate systems attached.

- the *link twist*, α_i, is the angle between adjacent joint axes about the line defining link i;
- the *joint offset*, d_i, is the offset along the joint axis of two adjacent links;
- the *joint angle*, θ_i, is the angle between adjacent links about the joint axis.

For A-pairs it is important to clarify the definitions of the joint angle and joint offset. The joint angle must be broken into two components, one fixed and one variable. The fixed component, θ_{fi}, refers the angle between adjacent links about the joint axis when the A-pair is in its home position. The variable component, θ_{vi}, is measured from the home position and it is this variable component that is used in Eqn. (1) to determine the separation of the fixed base and moving platform of the A-pair. The total joint angle is $\theta_i = \theta_{fi} + \theta_{vi}$. For the remainder of this paper it has been assumed that $\theta_{fi} = 0$ and therefore $\theta_i = \theta_{vi}$. The coupling of translation and rotation requires that the total joint offset also be broken into fixed and variable components. When working with A-pairs the parameter d_i refers to the the fixed component, that is, the distance along the joint axis between adjacent links when the joint is in the home position ($\theta_{iv} = 0$). The variable component of the joint offset is provided by Eqn. (1). The DH-parameters of the A-chain are illustrated in Fig. 3.

In addition to DH-parameters each link is assigned one reference coordinate system, and the assignment of this coordinate system depends on the two joint axes at the ends of the link. For the purposes of this description, each link i, $i = 1,\ldots,n$ describes a rigid link that lies on the common normal between axes i and $i+1$, irrespective of the actual shape of the physical link in the manipulator, which is irrelevant to the kinematic analysis. Let coordinate system i be denoted Σ_i. The origin of Σ_i established where link i intersects the joint axes i. The Z_i-axis of Σ_i points

along the i axis, the direction is arbitrary but, with experience, is selected to ease future calculations. The X_i-axis points along the common perpendicular towards the origin of Σ_{i+1}. If the axes i and $i+1$ intersect, the axis X_i is parallel to the normal of to the intersecting axes, the direction is again selected to ease future calculations. The Y_i-axis is assigned to complete the right-handed coordinate system. This procedure works well for intermediate links, however the base and EE coordinate systems, Σ_0 and Σ_n respectively, are often selected to simplify calculations by setting as many DH-parameters to zero as possible. Fig. 3 shows the placement of two coordinate systems in an A-chain.

A-Chain Direct Kinematic Equations

Using homogeneous coordinates, a point in the EE reference frame, $\left[1,\, x',\, y',\, z'\right]^T$, can be transformed to the global reference frame, $\left[1,\, x,\, y,\, z\right]^T$, using

$$\begin{bmatrix} 1 \\ x \\ y \\ z \end{bmatrix} = \mathbf{D} \begin{bmatrix} 1 \\ x' \\ y' \\ x' \end{bmatrix}, \tag{4}$$

where $\mathbf{D}$ is the matrix form of the direct kinematic equations obtained from

$$\mathbf{D} = \mathbf{M_1 G_1} \ldots \mathbf{M_i G_i} \ldots \mathbf{M_n G_n}, \tag{5}$$

where

$$\mathbf{G}_i = \begin{bmatrix} 1 & 0 & 0 & 0 \\ a_i & 1 & 0 & 0 \\ 0 & 0 & \cos(\alpha_i) & -\sin(\alpha_i) \\ d_i & 0 & \sin(\alpha_i) & \cos(\alpha_i) \end{bmatrix}, \tag{6}$$

and

$$\mathbf{M}_i = \begin{bmatrix} 1 & 0 & 0 & 0 \\ 0 & \cos(2\theta_i) & -\sin(2\theta_i) & 0 \\ 0 & \sin(2\theta_i) & \cos(2\theta_i) & 0 \\ \rho\sin(\theta_i) & 0 & 0 & 1 \end{bmatrix}, \tag{7}$$

recalling the earlier assumption that $\theta_{fi} = 0$ for the work presented in this paper. Note that $2\theta_i$ has been substituted for θ_i in order to eliminate fractions. The matrix $\mathbf{G}_i$ contains the link and joint parameters that do not change as the joint is actuated and the matrix $\mathbf{M}_i$ contains the joint variables that change as the joint moves.

Eqn. (5) is used to find the position and orientation of the manipulator EE when provided with the DH-parameters at any instant. This is a solution to the direct kinematics problem for any serially connected A-chain comprising any number, n, of A-pairs. The matrices used to obtain $\mathbf{D}$ are also used as part of the algorithm used to solve the inverse kinematics problem.

INVERSE KINEMATICS OF A-CHAINS

Solving the inverse kinematics problem for a kinematic chain involves determining the joint variables that place the EE of the manipulator in a desired pose. A complete solution to the inverse kinematics problem finds all sets of joint variables that achieve the desired EE pose. The algorithm for the inverse kinematics of A-chains is based on an algorithm for six-jointed serial manipulators with revolute joints presented by Pfurner [9] and Husty, Pfurner and Schröcker [10] that employs a technique called kinematic mapping to map displacements in a three dimensional Euclidean space, E_3, to a point in a homogeneous seven dimensional projective space. This section provides an overview of the kinematic mapping technique and shows how it is used in the algorithm for solving the inverse kinematics problem for A-chains.

It is important to note that for the purposes of this paper self-collisions have been ignored. Self-collisions occur when the physical elements that make up the manipulator collide with one another, preventing further motion. The self-collisions may occur between links in the chain or within the A-pair itself when the legs of the A-pair collide with one another, preventing further rotation (joint limits). When self-collisions are considered some solutions to the inverse kinematics problem must be discarded because they are not reachable by the actual manipulator. The inclusion of self-collision checking and joint limits to the inverse kinematics algorithm are topics for future research.

Kinematic Mapping

The algorithm for the inverse kinematics of serial chains used in this paper requires an understanding of the concept of the *kinematic mapping of displacements*. Kinematic mapping is the mapping of distinct rigid body displacements in E_3 to distinct points in a seven-dimensional projective space called the *kinematic image space*, P^7. Points in the image space are described by eight homogeneous coordinates $(x_0, x_1, x_2, x_3, y_0, y_1, y_2, y_3)$ called *Study parameters* [11–15]. Though every displacement in Euclidean space can be represented by a unique point in P^7 the opposite, that each unique point in P^7 represents a displacement, is not true. In order to represent a real displacement in Euclidean space the set of Study parameters must lie on the seven dimensional quadric

$$x_0y_0 + x_1y_1 + x_2y_2 + x_3y_3 = 0, \tag{8}$$

which is called the *Study Quadric*. Additionally, any set of Study parameters containing the generator space $x_0 = x_1 = x_2 = x_3 = 0$ satisfies Eqn. (8) but does not represent a real displacement because all of the Euler parameters that represent orientation would be zero, a situation with no physical meaning. This special generator space is called the *exceptional generator*. [1]

A displacement in E_3 can be described by a transformation matrix, $\mathbf{T}$, of the form

$$\mathbf{T} = \begin{bmatrix} 1 & 0 & 0 & 0 \\ d_1 & a_{11} & a_{12} & a_{13} \\ d_2 & a_{21} & a_{22} & a_{31} \\ d_3 & a_{31} & a_{32} & a_{33} \end{bmatrix}, \tag{9}$$

where the vector $\begin{bmatrix} d_1 & d_2 & d_3 \end{bmatrix}^T$ describes the position of the origin of the transformed coordinate system in the fixed reference coordinate system and the lower right 3×3 sub-matrix containing a_{ij} terms is a proper orthogonal matrix describing the orientation of the transformed coordinate system with respect to the fixed reference coordinate system. To transform the Euclidean displacement to a point in P^7 the first four Study parameters are obtained by one of the following ratios (using the elements of the matrix in Eqn. (9)):

$$\begin{aligned} x_0 : x_1 : x_2 : x_3 &= 1 + a_{11} + a_{22} + a_{33} : a_{32} - a_{23} \\ &\quad : a_{13} - a_{31} : a_{21} - a_{12} \\ &= a_{32} - a_{23} : 1 + a_{11} - a_{22} - a_{33} \\ &\quad : a_{12} + a_{21} : a_{31} + a_{13} \\ &= a_{13} - a_{31} : a_{12} + a_{21} \\ &\quad : 1 - a_{11} + a_{22} - a_{33} : a_{23} + a_{32} \\ &= a_{21} - a_{12} : a_{31} + a_{13} \\ &\quad : a_{23} + a_{32} : 1 - a_{11} - a_{22} + a_{33}. \end{aligned} \tag{10}$$

For some orientations one or more, but not all, of the preceding ratios will produce $[0:0:0:0]$. The ratios containing non-zero terms will all be equivalent and any of these non-zero ratios may be used [9]. The remaining Study parameters are found by

$$\begin{aligned} y_0 &= \tfrac{1}{2}(d_1 x_1 + d_2 x_2 + d_3 x_3), \\ y_1 &= \tfrac{1}{2}(-d_1 x_0 + d_3 x_2 - d_2 x_3), \\ y_2 &= \tfrac{1}{2}(-d_2 x_0 - d_3 x_1 + d_1 x_3), \\ y_3 &= \tfrac{1}{2}(-d_3 x_0 + d_2 x_1 - d_1 x_2), \end{aligned} \tag{11}$$

where the d_i terms are defined in Eqn. (9).

[1] In E_3 a generator of a quadric is a line of which all points on that line also lie on the quadric [16, 17]. The equivalent in P^7 is a hyperspace (a 3-plane [14, 15]) of which all points in the hyperspace also lie on the quadric. The exceptional generator is a generator space of the Study Quadric that does not represent a real displacement while all other generators do, hence the name exceptional generator.

It is possible to obtain the transformation matrix, $\mathbf{T}$, corresponding to a set of Study parameters by substituting the Study parameters into the matrix

$$\mathbf{T} = \Delta^{-1} \begin{bmatrix} \Delta & 0 & 0 & 0 \\ l & x_0^2 + x_1^2 - x_2^2 - x_3^2 & 2(x_1x_2 - x_0x_3) & 2(x_1x_3 + x_0x_2) \\ m & 2(x_1x_2 + x_0x_3) & x_0^2 - x_1^2 + x_2^2 - x_3^2 & 2(x_2x_3 - x_0x_1) \\ n & 2(x_1x_3 - x_0x_2) & 2(x_2x_3 + x_0x_1) & x_0^2 - x_1^2 x_2^2 + x_3^2 \end{bmatrix}, \tag{12}$$

where $\Delta = x_0^2 + x_1^2 + x_2^2 + x_3^2$ and

$$\begin{aligned} l &= 2(y_0x_1 - y_3x_2 + y_2x_3 - y_1x_0), \\ m &= 2(y_3x_1 + y_0x_2 - y_1x_3 - y_2x_0), \\ n &= 2(-y_2x_1 + y_1x_2 + y_0x_3 - y_3x_0). \end{aligned}$$

A displacement in E_3 in a particular coordinate system is represented by a point in P^7. If the coordinate system is moved or transformed then the representation of the displacement changes in both E_3 and P^7. Pfurner [9] shows that the two important transformations are those in the base coordinate system, which results in a change of the fixed coordinate system, and in the moving coordinate system, which results in a change of the EE coordinate system. Each type of transformation has a different influence on the the Study parameters in P^7 and must be examined separately.

The coordinate transformation is conveniently described by a matrix, $\mathbf{T}$, with the corresponding Study parameters $(t_0, t_1, t_2, t_3, t_4, t_5, t_6, t_7)^T$ and the displacement being transformed (for example, the displacement from the manipulator base to the EE) is represented by matrix $\mathbf{A}$ and Study parameters $\mathbf{a} = (a_0, a_1, a_2, a_3, a_4, a_5, a_6, a_7)^T$. If the transformation occurs in the fixed coordinate system, such as moving the entire manipulator relative to the fixed base coordinate system, then the transformed Study parameters are given by $\mathbf{T}_b\mathbf{a}$, where $\mathbf{T}_b$ is the 8×8 matrix

$$\mathbf{T}_b = \begin{bmatrix} t_0 & -t_1 & -t_2 & -t_3 & 0 & 0 & 0 & 0 \\ t_1 & t_0 & -t_3 & -t_2 & 0 & 0 & 0 & 0 \\ t_2 & t_3 & t_0 & -t_1 & 0 & 0 & 0 & 0 \\ t_3 & -t_2 & t_1 & t_0 & 0 & 0 & 0 & 0 \\ t_4 & -t_5 & -t_6 & -t_7 & t_0 & -t_1 & -t_2 & -t_3 \\ t_5 & t_4 & -t_7 & t_6 & t_1 & t_0 & -t_3 & t_2 \\ t_6 & t_7 & t_4 & -t_5 & t_2 & t_3 & t_0 & -t_1 \\ t_7 & -t_6 & t_5 & t_4 & t_3 & -t_2 & t_1 & t_0 \end{bmatrix}. \tag{13}$$

If the transformation takes place in the moving coordinate system then the transformed Study parameters are given by $\mathbf{T}_m\mathbf{a}$,

where $\mathbf{T}_m$ is the 8×8 matrix

$$\mathbf{T}_m = \begin{bmatrix} t_0 & -t_1 & -t_2 & -t_3 & 0 & 0 & 0 & 0 \\ t_1 & t_0 & t_3 & -t_2 & 0 & 0 & 0 & 0 \\ t_2 & -t_3 & t_0 & t_1 & 0 & 0 & 0 & 0 \\ t_3 & t_2 & -t_1 & t_0 & 0 & 0 & 0 & 0 \\ t_4 & -t_5 & -t_6 & -t_7 & t_0 & -t_1 & -t_2 & -t_3 \\ t_5 & t_4 & t_7 & -t_6 & t_1 & t_0 & t_3 & -t_2 \\ t_6 & -t_7 & t_4 & t_5 & t_2 & -t_3 & t_0 & t_1 \\ t_7 & t_6 & -t_5 & t_4 & t_3 & t_2 & -t_1 & t_0 \end{bmatrix}. \tag{14}$$

To build $\mathbf{T}_b$ or $\mathbf{T}_m$ for a displacement described by a 4×4 matrix, for example $\mathbf{M}_i$, the form $\mathbf{T}_b(\mathbf{M}_i)$ is used, meaning the $\mathbf{T}_b$ matrix is populated by the Study parameters associated with the matrix $\mathbf{M}_i$.

Kinematic mapping enables the use of powerful algebraic geometry tools for analysis. One such tool is the constraint variety [18].

Constraint Varieties of A-Chains

The constraint variety of a manipulator defines the set of all points in P^7 (all possible sets of Study parameters) that are reachable by the manipulator EE. The constraint variety of a manipulator may be visualized as a subset of points on the Study Quadric in the kinematic image space. In the work presented here the constraint variety is represented algebraically by a set of polynomials, though in several cases in literature, such as [3, 9, 10, 19, 20], it is represented by the intersection of some geometric entity with the Study quadric. The set of all solutions to a system of polynomials is called a *variety* and hence the set of all points in P^7 obtainable by a manipulator is called a *constraint variety*. The constraint variety can be said to be the variety defined by the set of polynomials that result from the mechanical constraints. For the inverse kinematics algorithm presented in this paper the constraint varieties of 1A- and 2A-chains are required.

Analysis of mechanical systems that possess design or motion parameters described by angles involves equations containing trigonometric functions. Computer algebra systems are generally more efficient with algebraic equations than those containing trigonometric functions, therefore the method of tangent of the half-angle substitution is used. Tangent of the half-angle substitution is based on the trigonometric identities

$$\sin\phi = \frac{2\tan(\frac{\phi}{2})}{1+\tan^2(\frac{\phi}{2})},\ \cos\phi = \frac{1-\tan^2(\frac{\phi}{2})}{1+\tan^2(\frac{\phi}{2})},$$

where $\phi \neq (2k+1)\pi$ and $k \in \{0,1,\ldots\}$. Substitution of a new variable

$$u = \tan\left(\frac{\phi}{2}\right) \tag{15}$$

into the identities provides the following identities

$$\sin\phi = \frac{2u}{1+u^2},\ \cos\phi = \frac{1-u^2}{1+u^2}. \tag{16}$$

As noted by Pfurner [9] these identities define a mapping of the points of a unit circle parameterized by ϕ to the set of real numbers. The inverse mapping is given by

$$\phi = 2\tan^{-1}(u). \tag{17}$$

From these mappings it can be seen that when $u=0$ then $\phi=0$, when $u=1$ then $\phi=\frac{\pi}{2}$ and as u goes to infinity ϕ approaches π.

The Study parameters of matrix $\mathbf{M_i}$ in Eqn. (7) are found using Eqn. (10) and Eqn. (11) and, after using trigonometric identities to eliminate the $2\theta_i$ terms and tangent of the half-angle substitution to remove the trigonometric terms, can be simplified to

$$\begin{pmatrix} x_0 \\ x_1 \\ x_2 \\ x_3 \\ y_0 \\ y_1 \\ y_2 \\ y_3 \end{pmatrix} = \begin{pmatrix} 1-u_i^4 \\ 0 \\ 0 \\ 2u_i(1+u_i^2) \\ 2\rho u_i^2 \\ 0 \\ 0 \\ \rho u_i(u_i^2-u_i) \end{pmatrix}, \tag{18}$$

where $u_i = \tan(\theta_i/2)$. In the seven dimensional space P^7 with one joint variable the constraint variety is represented by six independent equations which are obtained by eliminating u_i from Eqn. (18). The intersection of the six equations in the following set describes the constraint variety of a single A-pair in the kinematic image space:

$$\begin{aligned} 1:&\ x_0y_0+x_1y_1+x_2y_2+x_3y_3 = 0, \\ 2:&\ x_1 = 0, \\ 3:&\ x_2 = 0, \\ 4:&\ y_1 = 0, \\ 5:&\ y_2 = 0, \\ 6:&\ x_3^2-4\rho^{-2}y_0^2-4\rho^{-2}y_3^2 = 0. \end{aligned} \tag{19}$$

The constraint variety of a single A-pair is the intersection of the four hyperplanes $x_1=x_2=y_1=y_2=0$, the quadric $x_3^2-4\rho^{-2}y_0^2-4\rho^{-2}y_3^2=0$ and the Study quadric.

There are multiple ways to obtain the Study parameters of a 2A-chain. One could obtain the matrix $\mathbf{D}$ from Eqn. (5) with $i=2$, obtain the Study parameters in terms of the two joint variables

u_1 and u_2 and eliminate them to obtain the set of five independent equations whose intersection represents the 2A-chain constraint variety. Another method uses the matrix in Eqn. (14) to transform the Study parameters in Eqn.s (19). The transformed equations are obtained by substituting $\mathbf{x}'$ for $\mathbf{x}$ into the equations of the constraint variety for the single A-joint where $\mathbf{x}' = \mathbf{T}_m(\mathbf{G}_i)\mathbf{x}$ and the vectors $\mathbf{x}$ and $\mathbf{x}'$ are $\begin{bmatrix} x_0 & x_1 & x_2 & x_3 & y_0 & y_1 & y_2 & y_3 \end{bmatrix}$ and $\begin{bmatrix} x'_0 & x'_1 & x'_2 & x'_3 & y'_0 & y'_1 & y'_2 & y'_3 \end{bmatrix}$ respectively. The second A-pair is introduced into the model using the matrix $\mathbf{M}_{i+1}$. The set of equations parameterized in terms of the u_{i+1} describing the constraint variety of the 2A-chain are found by substituting $\mathbf{x}''$ for $\mathbf{x}'$ into the equations of the previous step (with link i already accounted for), where $\mathbf{x}'' = \mathbf{T}_m(\mathbf{M}_{i+1})\mathbf{x}'$. Elimination of the u_{i+1} term yields the set of five equations whose intersection is the 2A-chain constraint variety. Five equations are required to describe the constraint variety of a 2A-chain in P^7. The set of five equations, whose intersection is the 2A-chain constraint variety, are:

$$
\begin{aligned}
1: \quad & x_0y_0 + x_1y_1 + x_2y_2 + x_3y_3 = 0, \\
2: \quad & a_1x_1^2 + a_1x_2^2 + 2al_1x_1y_1 + 2al_1x_2y_2 = 0, \\
3: \quad & al_1^2x_0^2 - x_1^2 - x_2^2 + al_1^2x_3^2 = 0, \\
4: \quad & \rho^{-2}\left(4x_1y_2y_3 - 4x_2y_1y_3 - 2al_1a_1x_1x_3y_2 \right. \\
& \left. + 2al_1a_1x_2x_3y_1\right) - al_1x_0x_2x_3 = 0, \\
5: \quad & \rho^{-2}\left(2al_1^3a_1y_0^2 + 2al_1a_1y_1^2 + 2al_1a_1y_2^2 \right. \\
& + 2al_1^3a_1y_3^2 + \left(al_1^4a_1^2 + a_1^2\right)x_1y_1 \\
& \left. + \left(al_1^4a_1^2 + a_1^2\right)x_2y_2\right) + 2al_1^2x_1y_1 \\
& + 2al_1^2x_2y_2 + al_1^2a_1x_0x_1 = 0.
\end{aligned}
\tag{20}
$$

In Eqn.s (20), al_i describes the DH-parameter α_i after tangent of the half-angle substitution is used to transform trigonometric terms. The constraint variety is the intersection of three quadrics and one cubic with the Study quadric. The constraint variety of the 2A-chain is essential to the algorithm for solving the inverse kinematics problem for 4A-chains.

Algorithm for the Inverse Kinematics of 4A-Chains

The algorithm for the inverse kinematics of 4A-chains presented in this section is adapted from an algorithm for the inverse kinematics of 6R-chains by Pfurner [9, 10, 19].

In Pfurner's algorithm for the 6R-chain inverse kinematics algorithm one knows where the base coordinate system of the manipulator is located as well as the position and orientation of the EE (assuming the selected EE is in the workspace of the manipulator). The serial chain is theoretically broken into two sub-chains: the left chain which includes the original base of the full chain and a virtual end effector, EE_L, at the theoretical break where the third link meets the fourth joint; and the right chain which contains the original chain's EE and a virtual end effector, EE_R, at the theoretical break. The labeling of the chains as left and right comes from [9] and [10] because the figures showing the sub-chains show the base sub-chain being on the left hand side of the image and the EE sub-chain being on the right hand side. The EE of the original unbroken chain is modelled as the base of the right chain and it is placed in the desired EE pose. The algorithm now determines the sets of joint variables (θ_i values) that maintain the original, continuous serial chain (keeps EE_L and EE_R coincident) by computing the intersection of the constraint varieties of the left and right 3R-chains in the kinematic image space.

The algorithm for the inverse kinematics of 4A-chains parallels that of 6R-chains, however the manipulator is theoretically broken into two-jointed chains as opposed to three-jointed chains. The remainder of this section outlines the algorithm in more detail.

Breaking the Chain. The inverse kinematics problem for a 4A-manipulator involves finding all sets of joint variables (u_1, u_2, u_3, u_4, after tangent of the half-angle substitution) that place the EE in a desired pose. For a real solution to exist the target pose, Σ_{target}, represented by matrix $\mathbf{EE}_T$, must be within the reachable workspace of the manipulator. The first step of the algorithm is to theoretically break the 4A-manipulator, illustrated in Fig. 4, into two 2A-chains. The break may be made anywhere on link 2 of the 4A-manipulator, however it is convenient to make the break at the 'fixed' base of the third joint in the 4A-manipulator, at the origin of coordinate system Σ_2 of the full chain. The 2A-chain containing the base of the original 4A-manipulator is called the left chain and the EE of the left chain, Σ_L, is established at the break in the chain. The 2A-chain containing the EE of the original 4A-manipulator is called the right chain and the EE of the right chain, Σ_R, is established at the break in the chain. When the 4A-manipulator is unbroken Σ_L and Σ_R are coincident with Σ_2. The left chain contains Links and Joints 1 and 2. The base of the left chain, Σ_{0L}, remains the same as the base of the original 4A-manipulator, Σ_0. The right chain contains Links and Joints 3 and 4. The base of the right chain, Σ_{0R}, is established as Σ_{target} which is known and fixed relative to Σ_0. The order of the joints in the right serial 2A-chain is Joint 4 followed by Joint 3 of the original chain.

By modifying the constraint variety of the 2A-chain, represented by Eqn.s (20), the constraint varieties for the left and right chains are obtained. For the purposes of this paper the assumption has been made that Σ_0 is coincident with the universal coordinate system. If this not the case, the offset from the universal reference frame must be accounted for by a transformation in the base coordinate system. That being said, the constraint variety for the left chain is obtained by accounting for the second link in the 2A-chain constraint variety. This is done by substituting $\mathbf{x}'$ for $\mathbf{x}$ into Eqn.s (20), where $\mathbf{x}' = \mathbf{T}_m(\mathbf{G}_2)\mathbf{x}$. The primes are merely used for bookkeeping and can be eliminated once the substitutions are complete. The left 2A-chain constraint variety is represented by the intersection of the resulting five equations.

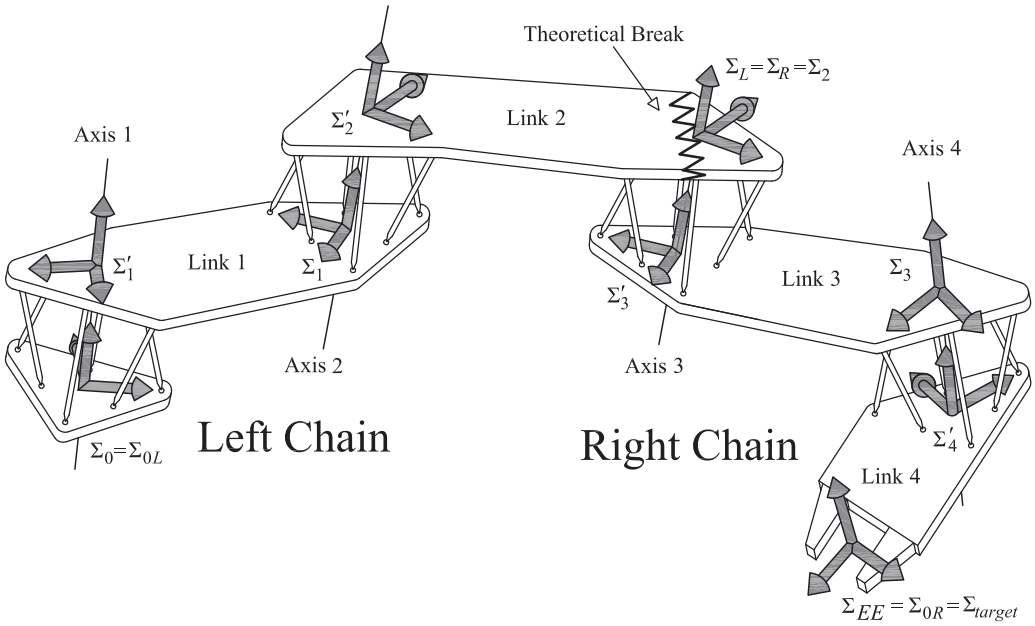

FIGURE 4. 4A-manipulator showing the theoretical break between the left and right 2A-chains.

Obtaining the constraint variety of the right chain is similar to the left chain, however a few additional steps are required. Comparing the right chain with the 2A-chain used to obtain the constraint variety represented by Eqn.s (20) it can be seen that the DH-parameters are obtained in the opposite directions relative to the coordinate frames attached to the links, therefore $-a_3$ and $-al_3$ must be substituted for a_1 and al_1 respectively. Unlike the left chain, it is not possible to assume Σ_{0R} coincides with Σ_0 and this must be accounted for by transforming from Σ_{target} to Σ_0 in the fixed coordinate system using the target pose matrix $\mathbf{EE}_T$ and the fact that Σ_{0R} is not at the base of the first A-pair, but at the end of the the last link in the 4A-chain. The geometry of the last link is defined by the matrix $\mathbf{G}_4$. To get from the Σ_0 to the base of the right 2A-chain the matrix $\mathbf{A}$ is used such that $\mathbf{A} = \mathbf{EE}_T\mathbf{G}_4^{-1}$. The inverse of $\mathbf{G}_4$ is used because the link is approached from the opposite direction compared to how it is defined for the direct kinematics of the full 4A-chain.

The Study parameters of the matrix $\mathbf{A}$ are obtained from Eqn. (10) and Eqn. (11) and the transformed equations of the constraint variety are obtained by substituting $\mathbf{x}'$ for $\mathbf{x}$ into in Eqn.s (20), where $\mathbf{x}' = \mathbf{T}_b(\mathbf{A})\mathbf{x}$. Notice that the transformation occurs in the base coordinate system. The fixed offset of the third joint has not yet been accounted for. This is done by substituting $\mathbf{x}''$ for $\mathbf{x}'$ into the set of equations obtained in the previous step, where $\mathbf{x}''$ is found from $\mathbf{x}'' = \mathbf{T}_m(\mathbf{G}'_3)\mathbf{x}'$ and $\mathbf{G}'_3$ is obtained using Eqn. (6) with $a_i = \alpha_i = 0$ and $d_i = -d_3$. The primes can now be removed from the resulting set of equations and the intersection of the five equations is the constraint variety of the right 2A-chain. The constraint variety of the right 2A-chain is dependent on the target EE pose for the 4A-manipulator, whereas the left 2A-chain constraint variety is unchanged if the Σ_{target} is changed.

Intersecting the Constraint Varieties. The goal of the inverse kinematics algorithm is to find all sets of joint variables that keep Σ_L and Σ_R coincident and therefore maintain an unbroken 4A-manipulator with the EE in the target pose. This is modelled as the intersection of the constraint varieties of the left and right 2A-chains.

The Study quadric is common to both constraint varieties and therefore the intersection of the two constraint varieties can be viewed as the intersection of eight equations with the Study quadric. The unknowns in the set of nine equations are the eight Study parameters. The equations are normalized by dividing all of the equations by one of the equations (normalize using the equation for the Study parameter that has been set to unity *i.e.* if using $x_0 = 1$. This can safely be done because the exceptional generator has been excluded. This yields an over determined set of nine equations in seven unknowns. In general there are no solutions to this over determined system, but because of the method of obtaining this set of equations there is at least one real solution for a target pose within the 4A-manipulator workspace.

Obtaining a general solution to the intersection problem proves to be difficult due to the size and degree of the equations. There exist many possible algebraic and numerical methods to

solve the intersection problem, however the effectiveness of the techniques may vary depending on the speed, accuracy and precision required, as well as the manipulator configuration and target EE pose. The method employed for specific numerical examples herein involves systematically eliminating variables until a univariate polynomial is obtained. Some equations are linear in terms of certain Study parameters or become linear when combined with other equations.

Seven of the nine equations are used to eliminate variables until a univariate polynomial is obtained. From this univariate polynomial several roots are obtained and back substitution is used to reveal the sets of Study parameters that satisfy the seven equations. Each set of Study parameters is tested in the remaining two equations and those which satisfy all nine equations represent the displacement from Σ_0 to the coincident Σ_L and Σ_R. In the numerical examples tested exactly one solution was obtained for the inverse kinematics problem for all 4A-manipulators. It has not been generally proven that there is only one solution to the 4A-manipulator inverse kinematics problem, however the fact that the general 4R-manipulator has only one solution [21] suggests it may be true.

Obtaining the Joint Variables. The sets of Study parameters obtained from the intersection of the left and right constraint varieties describe the pose of the coincident Σ_L and Σ_R with respect to Σ_0. In order to obtain the four joint variables of the 4A-manipulator the inverse kinematic problem for the two 2A-chains must be solved.

For the left 2A-chain the pose of Σ_L is described by $\mathbf{EE}_L = \mathbf{M}_1\mathbf{G}_1\mathbf{M}_2\mathbf{G}_2$. Obtaining the Study parameters of $\mathbf{EE}_L$ yields a set of eight equations in the two unknown joint variables u_1 and u_2. The equations are now set equal to the set of Study parameters obtained in the intersection problem resulting in a set of seven equations in two unknowns (u_1 and u_2). Once again, in general there is no solution because the system of equations is over determined, but due to the nature of the problem at least one real solution exists if a real solution was obtained when intersecting the constraint varieties (*i.e.* the target EE pose is within the manipulator workspace). Solving two of the equations provides many solutions which are tested in the remaining five equations. The sets of joint variables that satisfy all seven equations are the solutions. It is believed that like 2R-chains there is in general only one solution.

The procedure for obtaining u_3 and u_4 from the right 2A-chain is similar to that for obtaining the first two joint variables, after some initial pre-processing. Substituting the Study parameters obtained from the constraint variety intersection problem into the matrix of Eqn. (12) provides a transformation matrix, $\mathbf{T}_{EE_R}$, describing Σ_R relative to Σ_0. It is desired to find a matrix, $\mathbf{EE}_{T-relative}$, that describes Σ_{target} relative to Σ_R. This is achieved by $\mathbf{EE}_{\mathrm{T-relative}} = \mathbf{T}_{EE_R}^{-1}\mathbf{EE}_T$. The transformation from Σ_R to Σ_{EE} given by $\mathbf{T}_R = \mathbf{M}_3\mathbf{G}_3\mathbf{M}_4\mathbf{G}_4$ is a function of u_3 and u_4. Obtaining the Study parameters of $\mathbf{EE}_{\mathrm{T-relative}}$ and $\mathbf{T}_R$ using Eqn. (10) and Eqn. (11) and normalizing produces a set of seven equations and two unknowns that can be solved in a similar manner to left 2A-chain yielding the joint variables u_3 and u_4.

With the joint variables obtained for every intersection point between the left and right constraint varieties, the solution to the inverse kinematic problem is complete. The joint variables can be converted to angles using Eqn. (17) if desired.

CONCLUSIONS AND FUTURE WORK

This paper introduced a novel kinematic pair, the A-pair, using a specific configuration of the GDP. The self-motions inherent to the GDP throughout its entire workspace make it a failure as a parallel platform, however the well-defined one degree-of-freedom nature of the self-motions mean it can be utilized as a kinematic pair. Introducing this coupled motion into the joints of serial chains requires an investigation of the kinematics of A-chains and this paper has presented algorithms for solving both the direct and inverse kinematics problems.

The direct kinematic equations of A-chains are obtained by adapting well-known techniques to account for the coupling of translation and rotation in the A-pair. An algorithm for the inverse kinematics of 6R-chains is used as a template for solving the inverse kinematics problem of a 4A-chain. The mapping of Euclidean displacements to points in the kinematic image space is utilized to obtain the constraint varieties of 2A-chains. The inverse kinematics problem of a 4A-chain is solved by theoretically breaking the chain into two 2A-chains and intersecting the constraint varieties of the two shorter chains. This allows for the derivation of all sets of joint variables that place the EE in a desired pose.

The research presented focuses primarily upon the kinematics of A-chains and represents the begining of the investigation of this novel kinematic pair. Some topics for future research include: examining the kinematics of chains with different numbers of joints with the inverse kinematics of a 6A-manipulator being a major goal; investigating the rigidity of A-pairs relative to R-pairs; determining the limits of the self-motions of the A-pair by introducing self-collisions into the analysis; developing a method of actuating and controlling the self-motions of the A-pair; comparing the the reachable and dextrous workspaces of R-chains and A-chains; and investigating the forces and dynamics of A-manipulators. This list is by no means exhaustive but represents a good starting point for further research in the area of A-pairs and A-chains.

ACKNOWLEDGMENT

It is important to thank everyone at the Institute for Geometry and CAD at the University of Innsbruck especially Manfred

Husty, Martin Pfurner, Hans-Peter Shröcker and Dominic Walter for their continued guidance and assistance in the research of A-pairs and A-chains.

REFERENCES

[1] Griffis, M., and Duffy, J., 1993. Method and apparatus for controlling geometrically simple parallel mechanisms with distinctive connections. U.S. Patent Number: 5,179,525.

[2] Karger, A., and Husty, M., 2007. "Classification of all self-motions of the original Stewart-Gough platform". *Computer-Aided Design,* ***30***(3), pp. 205–215.

[3] Husty, M., and Karger, A., 2002. "Self motions of Stewart-Gough platforms, an overview". In Proceedings of the workshop on fundamental issues and future research directions for parallel mechanisms and manipulators, pp. 131–141.

[4] Husty, M., and Karger, A., 2000. "Self-motions of Griffis-Duffy type parallel manipulators". In Proceedings of ICRA '00 IEEE International Conference on Robotics and Automation, pp. 7–12.

[5] Robinson, J., 2008. "Direct and inverse kinematics of a new class of parallel-serial hybrid manipulator". Master's thesis, Carleton University, Canada.

[6] Denavit, J., and Hartenberg, R., 1955. "A kinematic notation for lower-pair mechanisms based on matrices". *Journal of Applied Mechanics,* ***77***, pp. 215–221.

[7] Craig, J., 2005. *Introduction to Robotics Mechanics and Control*. Pearson Prentice Hall, Upper Saddle River, NJ, USA.

[8] Shigley, J., and Uicker, J., 1995. *Theory of Machines and Mechanisms*. McGraw-Hill, Inc., New York, NY, USA.

[9] Pfurner, M., 2006. "Analysis of spatial serial manipulators using kinematic mapping". PhD thesis, University of Innsbruck, Austria.

[10] Husty, M., Pfurner, M., and Schröcker, H.-P., 2007. "A new and efficient algorithm for the inverse kinematics of a general serial 6R manipulator". *Mechanism and Machine Theory,* ***42***(1), pp. 66–81.

[11] Study, E., 1903. *Geometrie der Dynamen*. B.G. Teubner, Leipzig, Germany.

[12] Bottema, O., and Roth, B., 1979. *Theoretical Kinematics*. North-Holland Publishing Company, New York, NY, USA.

[13] McCarthy, J., 1990. *An Introduction to Theoretical Kinematics*. The MIT Press, Cambridge, MA, USA.

[14] Selig, J., 1996. *Geometrical Methods in Robotics*. Springer, New York, NY, USA.

[15] Selig, J., 2005. *Geometric Fundamentals of Robotics*. Springer, New York, NY, USA.

[16] Hilbert, D., and Cohn-Vossen, S., 1952. *Geometry and the Imagination*. Chelsea Publishing Company, New York, NY, USA.

[17] Semple, J., and Kneebone, G., 1952. *Algebraic Projective Geometry*. Oxford at the Clarendon Press, Oxford, UK.

[18] Cox, D., Little, J., and O'Shea, D., 1997. *Ideals, Varieties and Algorithms: An Introduction to Computational Algebraic Geometry and Commutative Algebra*. Springer, New York, NY, USA.

[19] Husty, M., Pfurner, M., Schröcker, H.-P., and Brunnthaler, K., 2007. "Algebraic methods in mechanism analysis and synthesis". *Robotica,* ***25***, pp. 661–675.

[20] Brunnthaler, K., 2007. "Synthesis of 4R linkages using kinematic mapping". PhD thesis, University of Innsbruck, Austria.

[21] Manseur, R., and Doty, K., 1992. "A complete kinematic analysis of four-revolute-axis robot manipulators". *Mechanism and Machine Theory,* ***27***(5), pp. 575–586.